

An innovative detector for X-ray beams made of polyethylene terephthalate built in a 3D printer

Daniel F. Gomes¹, Edvane B. Silva¹, and Luiz A. P. Santos^{2,3,*}

¹UFPE, Brazil

²CRCN-NE/CNEN, Brazil

³SCIENTS, Brazil

(*) lasantos.scients@gmail.com

Abstract—3D printers have been increasingly used to create different objects and tools for the most diverse areas of knowledge. In this paper, we bring results of the response of an X-ray detector that was made on a 3D printer with polyethylene terephthalate glycol (PET-G) material. The manufacturing process has practically two steps, which consists of building a composite of two materials: a build-up cap made of PET-G; and a semiconductor film made of carbon-doped PET. The experimental methods performed were basically to compare the signals from the new PET-based X-ray detector with the signals from typical detectors. Clinical X-ray beams were used to test such an innovative detector. Two X-ray tube parameters were varied to analyse the response of the PET-based X-ray detector: potential (kV) and workload (mAs). The study points out the PET-G detector works and is easy to manufacture, although the signal is weaker than a typical semiconductor detector. Also, the noise signal is at least one order of magnitude smaller than silicon detectors. Furthermore, the density of PET is almost equivalent to human tissue, which is an advantage for dosimetry in phantoms. Finally, such a detector could become an option for X-ray beams in the near future.

Keywords — Polyethylene terephthalate, X-ray, Detector.

I. INTRODUCTION

SINCE the last century, some international institutions of both radiological protection and health [1-2], have been warning about some possible radiological accidents due to unnecessary radiation doses or overdoses in patients undergoing medical radiodiagnosis. In fact, these types of events have already happened and some researchers are looking to develop new detectors or dosimetry systems to be applied in radiodiagnosis. Furthermore, the modern digital radiology equipment itself operates with high dose rates [3], although in this type of equipment the patient is usually exposed to radiation in a short time when submitted to radiography exams, for example. Also, there are several researches in the dosimetry area that use detectors inserted inside human body simulator [4] (e.g. Alderson Random anthropomorphic phantom) to avoid performing measurements in humans (in vivo dosimetry) that could evidently be harmful to patients.

Regarding the methods that use numerical dosimetry with

phantoms, the detectors are not always made with equivalent tissue material, such as silicon, which is widely used in semiconductor detectors. Furthermore, it is known that the manufacturing process of the silicon detector is complex and in some cases it can take long time to build it. However, 3D printers have been increasingly used to create different objects and tools for the most diverse areas of knowledge, among which we can exemplify: mechanical engineering, medicine, information technology, in addition to objects such as toys, souvenirs, etc. For the reasons explained above, we were motivated to create an innovative X-ray detector, which is built of polyethylene terephthalate Glycol (PET-G), for applications in X-ray beams for medical radiology.

II. MATERIAL AND METHODS

A. Building the PET detector

Firstly, PET material was chosen to build the X-ray detector due to the fact that it is the raw material for 3D printer. In this way, the PET itself becomes the detector's buildup cap. Furthermore, PET can be doped with carbon to become a semiconductor, which will provide the conduction of the current signal produced during irradiation. Fig. 1 shows an illustration of the detector manufactured on a 3D printer. Basically the detector is made in two steps: 1) PET-G chip and wires are impregnated on the edges; 2) a thin carbon-doped PET film is deposited onto the chip in the region between the two wires. The PET chip volume dimensions ($L \times W \times H$) can vary depending on the photon energy or desired output current. Therefore it can be from 0.1 cm^3 up to 1 cm^3 , for while.

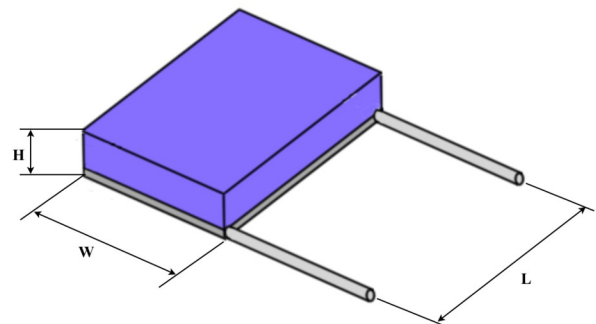


Fig. 1. Illustration of the PET X-ray detector: PET (orchid); carbon-PET semiconductor film (grey); metallic wire (silver).

B. Biasing the PET detector and instruments

The buildup cap has the purpose of increasing the electron rain due to the numerous interactions that occur there (see Fig. 15 in [5]). Actually, the voltage bias is for the carbon-PET semiconductor film and it is where the current generated by the electron rain will be conducted between the wires of the detector. The detector biasing circuit schematic is illustrated in Fig. 2. A 6430 source-meter, Keithley®, was used for biasing the detector with 20V in SVM mode (voltage-source and current-measurement). Although the detector can be biased with voltages between 5 and 35V, it was chosen the average value to improve the signal-to-noise ratio and avoid hysteresis in the detector's $I \times V$ curve. One way to characterize the PET X-ray detector is to trace its $I \times V$ curve on a semiconductor parameter analyzer, 4200A-SCS, Keithley®. Such a technique can also show us how much the PET detector is damaged by the accumulated radiation dose.

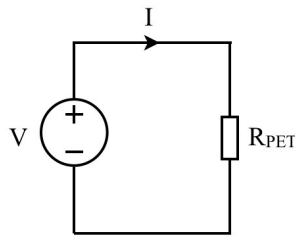


Fig. 2. Circuit schematic to bias the PET X-ray detector.

C. Testing the PET detector under X-ray beams

To perform tests with the PET-G detector, a clinical X-ray generator was used: Polymat 30/50 Plus, Siemens®. In the control panel of the clinical equipment it is possible to select the main X-ray tube parameters: 1) Exposure time (ms); 2) Potential (kV); 3) Workload (mAs). Table 1 displays the parameters and their respective selectable values. In order to compare the PET detector measurements with other types of semiconductor detectors, experiments were done varying the kilovoltage and the workload. For all experiments the X-ray pulse duration was held constant at 3200 ms. Experiments were performed using PET X-ray detectors with following dimensions: $1 \times 1 \times 0.3 \text{ cm}^3$. Each point on each graph in the results is to the average of two readings. Each experiment was repeated twice to check reproducibility. Fig. 3 illustrates the setup for carrying out the PET detector irradiation procedures.

D. Basic methods

First, the PET-G detector was analyzed under an optical coherence microscope, THORLABS®, to see if the carbon-doped PET film was uniform. Second, $I \times V$ curve of the device was analyzed to confirm that the detector behaves like a resistor, here called R_{PET} . Finally, under pulses of diagnostic X-rays, PET detector output signal measurements were made.

The first part of the irradiation procedures consisted in verifying how the PET detector responds to beams with different X-ray tube potentials. In this procedure, the workload

was varied for the following values: 100 mAs and 200 mAs. In order to have comparison with silicon based devices two additional experiments were done: 1) FQP20N06C MOSFET measurements; 2) ZTX851 NPN Bipolar Junction Transistor (BJT) measurements.

TABLE I
X-RAY TUBE PARAMETERS AND SELECTABLE VALUES

X-ray tube parameter	Selectable values
Potential (kV)	52, 63, 77, 82, 90, 102, 117, 125
Workload (mAs)	50, 62.5, 80, 100, 125, 160, 200, 250, 320
Pulse time (mS)	50, 100, 200, 400, 800, 1000, 1600, 2000, 3200

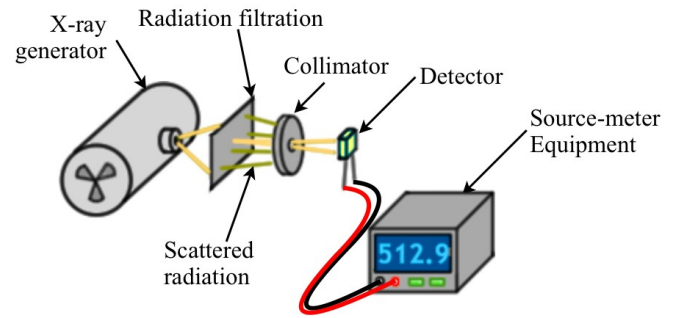


Fig. 3. Experimental setup for PET X-ray detector irradiation [5].

III. RESULT AND DISCUSSIONS

As shown in Fig. 4, the carbon-doped PET semiconductor film did not have uniformity in its deposition on the PET-G chip and, consequently, in its thickness within the region between the two wires. In addition to the deposition of the carbon-PET film not being perfect, the face of the PET-G chip itself is also not perfect, unlike the surface on the silicon crystal.

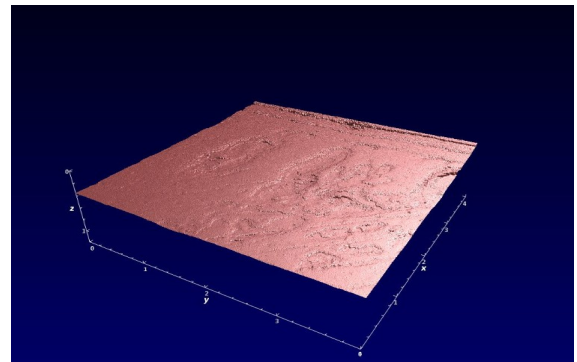


Fig. 4. An optical coherence tomography of a PET-G detector sample.

Fig. 5 shows the PET detector is like a $2.5 \pm 0.2 \text{ G}\Omega$ resistor. Furthermore, it appears to have a capacitance (to be studied later), as the behavior is not exactly a straight line. Prior to irradiating the PET detector samples, dosimetry of the X-ray pulses was performed with our reference detector, 10X5-6 ion chamber, Radcal®, to measure the dose rate of each X-ray tube potential in Table 1. The pulse dosimetry results are shown in Fig. 6.

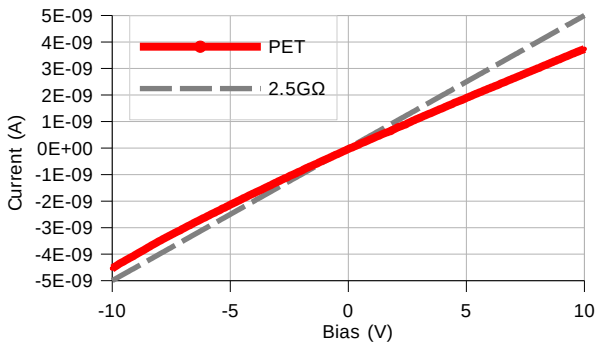


Fig. 5. I×V curve of a PET detector sample: $R_{PET}=2.5\pm 0.2\text{ G}\Omega$.

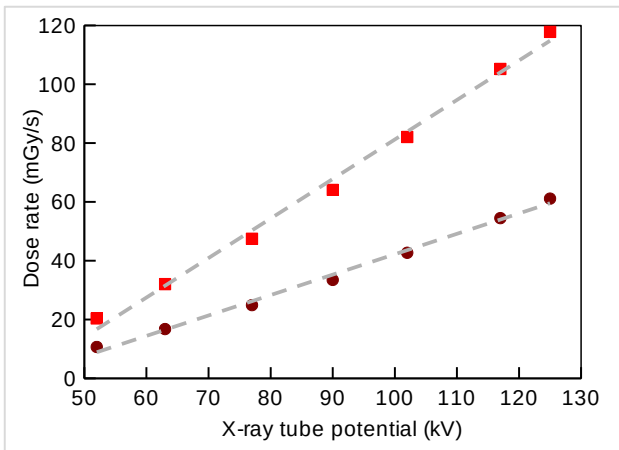


Fig. 6. Dose rate as a function of X-ray tube potential at the position where the PET detector was placed to perform measurements during irradiation: 100mAS (maroon); 200mAS (red).

The first comparison, which was made with a MOSFET, is shown in Fig. 7 and Fig 8. Note that, although the responses of each type of detector closely resemble the response of the reference detector, the signal produced by the PET detector is weaker than the signal produced by the MOSFET. Actually, if the latter is compared with other silicon semiconductor devices, a MOSFET has the weakest signal than a BJT or phototransistor, for example [6]. However, the PET detector signal is about 20-40 dB stronger than a typical ionization chamber. On the other hand, at room temperature, the noise signal produced by a PET detector is around 0.2 nA, whereas the signal from a silicon semiconductor device can vary between 2 nA and 20 nA, for example. That is, the noise in the silicon device is at least 20dB greater than the R_{PET} resistor.

Another comparison was made based on the effect of radiation on a BJT. Although the output signal of a BJT is 40-60 dB stronger than PET output signal when it is irradiated, a degradation in transistor gain systematically occurs [5]. It can be easily seen in Fig. 9 and Fig. 10 the effect of irradiation on the BJT and PET detector, respectively. One can observe that the transistor gain decreases and consequently the transistor output signal also decreases, whereas the PET detector output signal remains practically constant. Note that the PET detector received double the dose received by the BJT. PET samples were sequentially irradiated with a dose of approximately

7.86Gy (30 X-ray pulses of $\approx 262\text{ mGy}$) and no traces of degradation were measured by the source-meter. This total dose corresponds to about 7860 exposures (typical lung radiograph $\approx 1\text{ mGy}$) [1], i.e., the innovative detector could be inserted into a phantom to measure more than 7800 times the dose rate there.

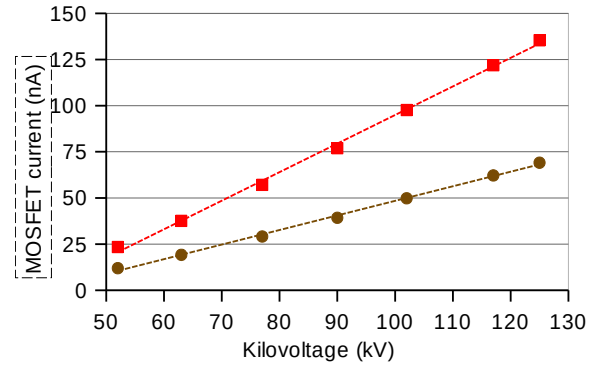


Fig. 7. MOSFET detector output signal as a function of X-ray tube potential, for workload of 100mAS (maroon), and 200mAS (red).

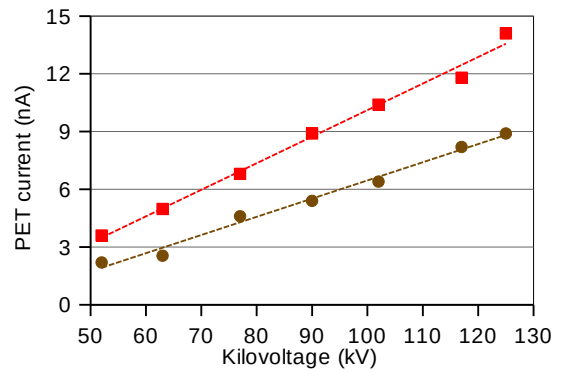


Fig. 8. PET detector output signal as a function of X-ray tube potential, for workload of 100mAS (maroon), and 200mAS (red).

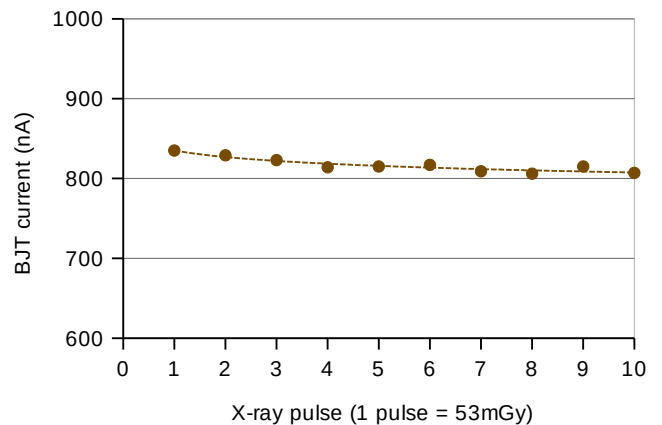


Fig. 9. BJT output signal after 10 X-ray pulses; $D = 530\text{ mGy}$.

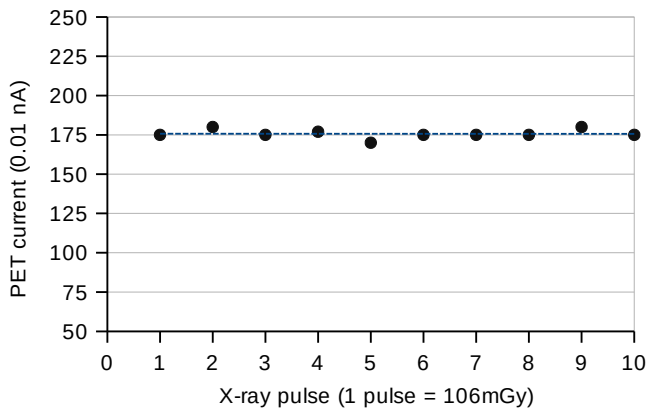


Fig. 10. PET detector output signal after 10 X-ray pulses; D = 1060 mGy.

IV. CONCLUSIONS

An innovative radiation detector for X-ray beams applied to radiodiagnosis was presented. The output signal of this new device is about 20dB weaker than a MOSFET, which is the weakest signal among silicon-based detectors. On the other hand, the PET detector has some advantages for using it as a detector in radiation beams. First of all, it is a device that can be easily manufactured by a 3D printer in a practical and fast way, unlike silicon semiconductor detectors. Second, the PET detector behaves like a typical resistor, which has a weaker noise signal than a silicon semiconductor at room temperature. One of the main advantages of PET detector is radiation hardness as it can be used repeatedly without degradation. Furthermore, the PET detector has a density that makes it equivalent to human tissue, which is an important feature for it to be usable inside phantoms. Also, it is important to point out that the device's semiconductor film between the wires is irregular, without impairing its functioning as a radiation detector. Finally, such a detector could become an option for X-ray beams in the near future.

ACKNOWLEDGMENT

The authors would like to thank the “Unidade de Diagnostico por Imagem” of the University Hospital (HC-UFPE/EBSERH) for the collaboration in the irradiation procedures. We also thank the company Sciens (contract 200313) and the Brazilian agency CNPq for financial support (grant 315017/2021-7).

REFERENCES

- [1] IAEA, “Applying radiation safety standards in diagnostic radiology and interventional procedures using X rays,” IAEA., Vienna, Austria, Safety Report Series, No. 39., Oct. 2006.
- [2] ICRP, “The 2007 Recommendations of the International Commission on Radiological Protection,” ICRP Publication 103, Vienna, Austria, Annals of the ICRP, 2007.
- [3] C. J. Martin, “Management of patient dose in radiology in the UK,” *Rad. Protec. Dosim.*, vol. 147, pp. 355–372, Nov. 2011, doi: 10.1093/rpd/ncr386.
- [4] G. Brix, U. Lechel, R. Veit, R. Truckenbrodt, G. Stamm, E. M. Coppenrath, J. Griebel, H. -D. Nagel, “Assessment of a theoretical formalism for dose estimation in CT: an anthropomorphic phantom study,” *Eur. Radiol.*, vol. 14, pp. 1275–1284, 2004, doi: 10.1007/s00330-004-2267-7.

- [5] L. A. P. Santos, “An Overview on Bipolar Junction Transistor as a Sensor for X-ray Beams Used in Medical Diagnosis” *Sensors*, vol. 22, no. 5, 1923, Mar. 2022, doi: 10.3390/s22051923.
- [6] C. P. V. Valença, L. C. Gonçalves Filho, A. N. Alves, M. A. Macedo, D. N. Souza, L. A. P. Santos, D. A. A. Santos, “The comparison of a thin-film ZnO nanodevice with silicon-based electronic devices for diagnostic X-ray beam detection,” *Radiation Effects and Defects in Solids*, vol. 177, pp. 642–654, June 2022. doi: 10.1080/10420150.2022.2073878